
*17th World Conference on Earthquake Engineering, 17WCEE*
*Sendai, Japan - September 13th to 18th 2020*

# ESTIMATION OF FUTURE POPULATION EXPOSURE TO SEISMIC HAZARD: A CASE STUDY OF ASIAN MEGACITIES

G. Mestav Sarica[(1)], T. Zhu[(2)(3)], T-C. Pan[(4)(5)]

[(1)] *Ph.D. Candidate, Institute of Catastrophe Risk Management, Nanyang Technological University, Singapore, gizem001@e.ntu.edu.sg*
[(2)] *Civil Engineer, Arup, Singapore, Tinger.Zhu@arup.com*
[(3)] *Formerly, Research Assistant, School of Civil & Environmental Engineering, Nanyang Technological University, Singapore*
[(4)] *Executive Director, Institute of Catastrophe Risk Management, Nanyang Technological University, Singapore, cpan@ntu.edu.sg*
[(5)] *Professor, School of Civil & Environmental Engineering, Nanyang Technological University, Singapore*

## *Abstract*

Exposure is a highly dynamic component of seismic risk; therefore, quantification of future exposure is an intricate task. As the world continues to urbanize, the estimation of population exposure to earthquakes becomes more crucial for risk assessment and management purposes. The urban population in Asian megacities, cities which have more than 10 million inhabitants, has been growing rapidly in recent years. Being situated in the vicinity of the North Anatolian Fault Zone, the megacity of Istanbul has been the focus of risk assessment studies especially after M 7.4 Kocaeli and M 7.2 Duzce earthquakes in 1999. Metro Manila and Jakarta, located in the Pacific Ring of Fire, are densely urbanized megacities which are also threatened by earthquakes. The main aim of this study is to estimate the future population exposure in these three megacities. For this purpose, the built-up area was projected for 2030 using a cellular automaton-based urban growth model SLEUTH. The name SLEUTH is an acronym for its six inputs which are slope, land use, excluded, urban extent, transportation and hillshade. Using the projected built-up area as ancillary data, the extrapolated census populations were disaggregated spatially based on the approach in the European Commission's Global Human Settlement Layer framework. Finally, probabilistic seismic hazard maps for 10% and 2% probabilities of exceedance in 50 years were overlaid with the population grids to obtain the population exposed to seismic risk. The results show that the urban growth trends of megacities are different as all have experienced different urbanization trends in the past. We found that the number of people subjected to MMI VIII (Moderate/Heavy) level for 10% probability of exceedance in 50 years is predicted increase from 10.3 million to 11.8 million in Jakarta, from 10.4 million to 12.3 million in Metro Manila, and from 13.2 million to 15.2 million in Istanbul by 2030. For 2% probability of exceedance in 50 years, the population subjected to MMI IX (High) level is predicted to increase from 9.8 million to 11.2 million in Jakarta, from 13.1 million to 15.5 million in Metro Manila, and 11.1 million to 12.7 million in Istanbul. As a result of following a spatio-temporal approach, we observed that the population subjected to different MMI levels show different growth trends in each megacity. While urban growth modelling has been used for risk assessment of other natural hazards, seismic hazard has not been the focus of many previous studies. Therefore, this study shows that projection of the built-up area and population exposed to seismic risk should be considered by decision-makers and urban planners for more complete risk assessment, management and mitigation strategies.

*Keywords: seismic exposure; population exposure; seismic risk assessment; urban growth modelling; cellular automata*



## 1. Introduction

Following the rapid urbanization, static risk assessment methods appear to be inadequate to reflect the pace of change in megacities which are complex systems [1]. Exposure is a highly dynamic component of seismic risk that varies across temporal and spatial scales [2]. Therefore, quantification of time-dependent exposure is critical for a complete risk assessment. Among all exposure elements, population has been regarded as the most important element since it represents the human dimension of risk [3]. Most of the previous studies have focused on past and/or present population potentially exposed to disasters [4-8]; however, the research on future predictions of population exposure remains limited due to the complexity involved. Moreover, although making predictions on exposure has been adopted widely for weather-related natural hazards [9-12], there is a limited number of studies which address future seismic exposure [13]. A common strategy used to estimate future exposure is to make temporal predictions that assumes all exposed people will be equally affected by possible disasters. Therefore, a challenging problem that arises in this domain is to make spatio-temporal predictions which would result in a different growth rate for each region/grid. The question then becomes how best to estimate the future population exposure to seismic hazard which can be utilized by policymakers, re/insurance industry and urban planners for more effective disaster risk reduction strategies.

Various scales (i.e. global, local, grid-based, etc.) have been used by different studies to quantify the exposure [4, 6, 14, 15]. Risk and exposure models developed by the re/insurance industry generally use the local data; however, there are limitations to access this level of data [16]. Thus, it may not be always possible for researchers to scrutinize the exposure trends, especially for developing countries. Global gridded population databases generally have low spatial resolutions [17-19] while the satellite images based on remote sensing provide relatively high-resolution information about land use and land cover (LULC). Furthermore, the expansion in built-up area are not considered by most of the population databases which results in the disaggregation of extrapolated census population to the same urban extent for different years.

In this study, we aim to estimate the future grid-based exposure by utilizing high-resolution open-source data, particularly focusing on the population exposed to seismic risk in the selected megacities. With this aim in mind, we followed a spatio-temporal approach to assess the changes from current exposure to future exposure in 2030 by utilizing a cellular automaton-based urban growth model SLEUTH. Using the future built-up area in 2030 as ancillary data for the disaggregation of extrapolated census population, which is overlaid on the seismic hazard maps, we calculated the number of people exposed to different Modified Mercalli Intensity (MMI) levels for 10% and 2% probabilities of exceedance in 50 years. The framework of our approach is demonstrated in Fig.1.

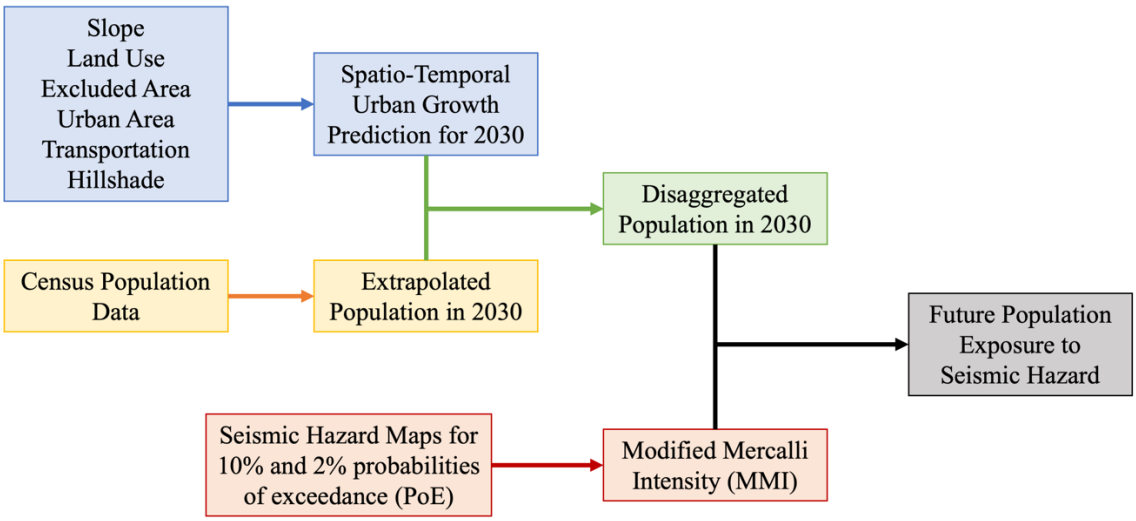


Fig. 1 – Framework for estimation of future population exposure to seismic hazard



© The 17th World Conference on Earthquake Engineering 



We selected three Asian megacities, namely Jakarta, Metro Manila and Istanbul, as case studies since Asia is one of the most earthquake-prone and urbanized regions in the world. Jakarta (651 $km^2$) and Metro Manila (636 $km^2$), located in the Pacific Ring of Fire, are densely urbanized megacities threatened by earthquakes. Jakarta is located on the northwestern coast of Java island which has been hit by recent earthquakes with magnitudes larger than 5. Metro Manila is also an earthquake-prone megacity while Mw 6.1 Luzon Earthquake has struck the Luzon island, home of Metro Manila in 2019. Being situated in the vicinity of the North Anatolian Fault Zone, Istanbul (5,461 $km^2$) has been the focus of risk assessment studies especially after the Mw 7.4 Kocaeli and the Mw 7.2 Duzce earthquakes in 1999. In fact, the recent Mw 5.7 Marmara earthquake has emphasized the necessity of taking measures for risk management in the city.

The key contribution of this work is mainly the framework it provides for future seismic exposure quantification in a systematic way to combine different methods in the literature which have previously been used for other purposes. While urban growth modelling has been utilized for topics related to urban planning, sustainability or environmental protection, we show that it could also be employed directly or to obtain ancillary data that could help urban planning policy and disaster risk management decisions. Although we have focused on seismic risk in this paper, our framework can be applied for risk management of other types of natural hazards.

## 2. Methods

### 2.1 Urban Growth Model

A cellular automaton-based urban growth model SLEUTH [20] was used for prediction of future built-up area in 2030. The name SLEUTH is an acronym for its six inputs: slope, land use, excluded area, urban area, transportation and hillshade. In this study, only urban/nonurban land use classification was used to obtain built-up area cells; therefore, land use is not an input for our model. Grid size (in Universal Transverse Mercator coordinate system) for the inputs is 30m for Jakarta and Metro Manila. On the other hand, 90m grids were used for Istanbul due to its larger total area. To obtain the slope (in percentage) and hillshade inputs, Digital Elevation Maps (DEM) (available at https://earthexplorer.usgs.gov/) were used. For urban area and excluded area (i.e. water bodies) inputs, Landsat Thematic Mapper (TM) images were processed with the help of semi-automatic classification plugin on QGIS [21]. SLEUTH requires at least four urban area inputs; hence, Landsat TM images corresponding to following years were used considering less cloud cover: Jakarta (1995, 2001, 2006 & 2018), Metro Manila (1995, 1999, 2009 & 2016) and Istanbul (1995, 2005, 2013 & 2018). The latest urban area maps (2018 for Jakarta and Istanbul, and 2016 for Metro Manila) were used to represent the present time. After three phases (coarse, fine and final) of calibration using Monte Carlo iterations on SLEUTH, best-fit urban growth coefficients were obtained for prediction. To determine the goodness of fit for each parameter set, we calculated the Lee-Sallee shape index values which are around 0.8 at the end of the calibration process for all megacities.

Employing the prediction mode of SLEUTH with business as usual scenario, urbanization probability of each grid in 2030 was obtained. In Fig.2, different shades of green and red demonstrate the urbanization probabilities while the urban extent of seed year (corresponding to latest urban input) is represented by yellow. The results reveal that each megacity shows different urban expansion patterns as all have experienced different urbanization trends in the past. For example, Istanbul shows an urban expansion towards the edges of the current urban extent due to the new infrastructural developments. There is a limited available land for urbanization in the core of the city as it has already been urban for a very long time. On the other hand, newly urbanized cells are filling up the gaps among current urban cells in Jakarta and Metro Manila. The maps showing probabilities of urbanization in 2030 were used as ancillary data for disaggregation of extrapolated census population in the next steps.



© The 17th World Conference on Earthquake Engineering 



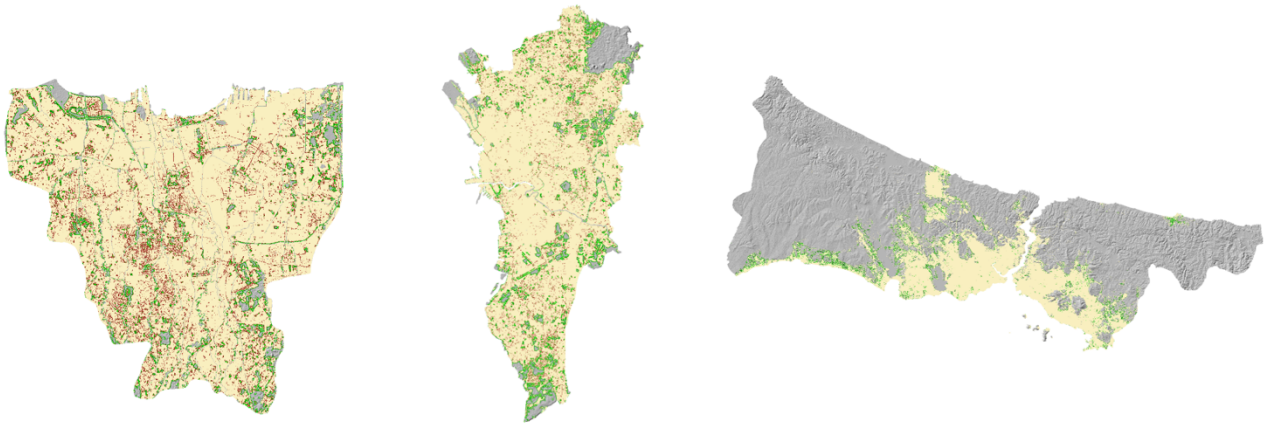

(a) Jakarta (b) Metro Manila (c) Istanbul

| Probability of Urbanization (%) | 50-60 | 60-70 | 70-80 | 80-90 | 90-95 | 95-100 | Urban Extent in Seed Year |
|---|---|---|---|---|---|---|---|

Fig. 2 – Urbanization probabilities of grids in 2030 (Maps not to scale)

## 2.2 Population Projection and Disaggregation

Population data were obtained for Level 2 administrative boundaries (available at https://gadm.org/) as illustrated in Fig.3 (i.e. 5 regions in Jakarta, 17 cities in Metro Manila and 39 districts in Istanbul) from Statistics Indonesia for Jakarta [22], Philippine Statistics Authority for Metro Manila [23] and Turkish Statistical Institute for Istanbul [24]. Census data are available for the regions in Jakarta and cities in Metro Manila while annual population data from the address-based population registration system are available for the districts in Istanbul. To predict population in 2030 for each megacity, linear regression was used to extrapolate the population data represented in Table 1. Before the extrapolations, trends of individual Level 2 populations and the availabilities for urbanization were scrutinized. It was observed that there is one district in Istanbul (i.e. Esenyurt) which has shown a drastic population increase (around 0.5 million) in 10 years. Since currently it does not have an available area for further urban expansion, its trend was not included in the linear regression. Therefore, its population in 2018 was assumed to stay constant in 2030. The total populations of Jakarta, Metro Manila and Istanbul were predicted to be around 12 million, 15.5 million and 17.6 million by 2030.

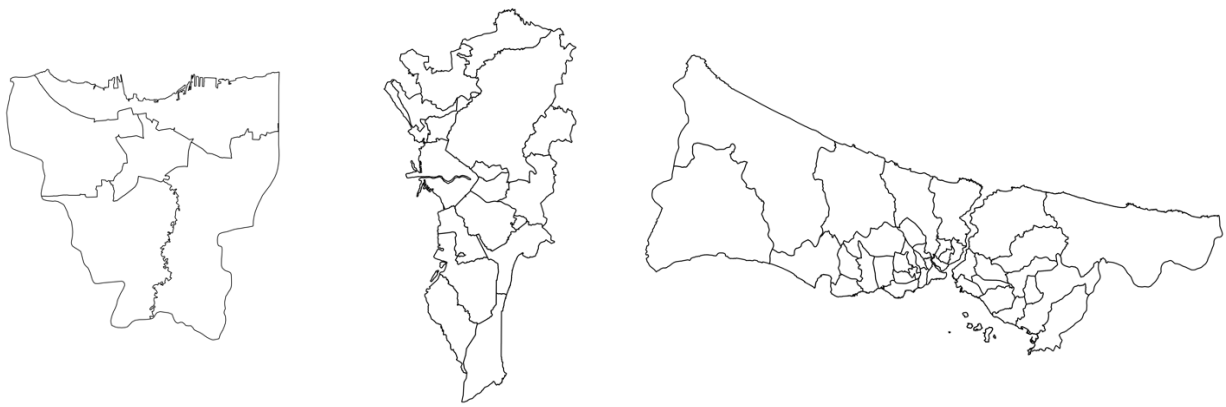

(a) Jakarta (b) Metro Manila (c) Istanbul

Fig. 3 – Level 2 administrative boundaries



© The 17th World Conference on Earthquake Engineering 



Table 1 – Population data and projections for 2030

| Years | Jakarta | Metro Manila | Istanbul |
|---|---|---|---|
| 1995 | - | 9,449,000 | - |
| 2000 | 8,385,600 | 9,931,000 | - |
| 2005 | 8,840,000 | - | - |
| 2007 | - | 11,548,000 | - |
| 2008 | - | - | 12,697,164 |
| 2009 | - | - | 12,915,158 |
| 2010 | 9,640,000 | 11,855,000 | 13,255,685 |
| 2011 | - | - | 13,624,240 |
| 2012 | - | - | 13,854,740 |
| 2013 | - | - | 14,160,467 |
| 2014 | - | - | 14,377,018 |
| 2015 | 10,150,000 | 12,878,000 | 14,657,434 |
| 2016 | - | - | 14,804,116 |
| 2017 | - | - | 15,029,231 |
| 2018 | - | - | 15,067,724 |
| 2030 | 11,995,840 | 15,479,147 | 17,632,929 |

During the population disaggregation, we utilized the approach in the European Commission's Global Human Settlement Layer framework [25]. For the estimation of present exposure, we extrapolated Level 2 populations to 2018 for regions Jakarta and 2016 for cities in Metro Manila while population data of districts in Istanbul are already available for 2018. Then, we simply divided the population values to the total number of built-up area grids to calculate the average population density in each Level 2 boundary (Fig.4). To allocate the people to newly urbanized cells in 2030, we assume that the population densities of newly urbanized cells in 2030 will not exceed the average population densities of present urban cells (2016 for Metro Manila and 2018 for Jakarta and Istanbul) in the same Level 2 boundary. For example, a newly urbanized cell with 80% probability of urbanization in 2030 will have a value of 80% of the population in a present urban cell in the same boundary.

After disaggregating population following our assumption, the aggregated populations of Istanbul and Metro Manila are found to be lower than population values that are predicted by linear regression for 2030. Thus, all cells were scaled by multiplying their population densities with the ratio of predicted total population (by linear regression) to aggregated total population (considering probabilities of newly urbanized cells). On the other hand, a different approach was employed for Jakarta since the aggregated population was slightly higher than what was predicted by linear regression. Hence, only newly urbanized cells were scaled to adjust the aggregated population assuming the population density of present urban cells cannot decrease in the future. In Fig.4, present and future population density maps for all megacities are represented.



© The 17th World Conference on Earthquake Engineering 




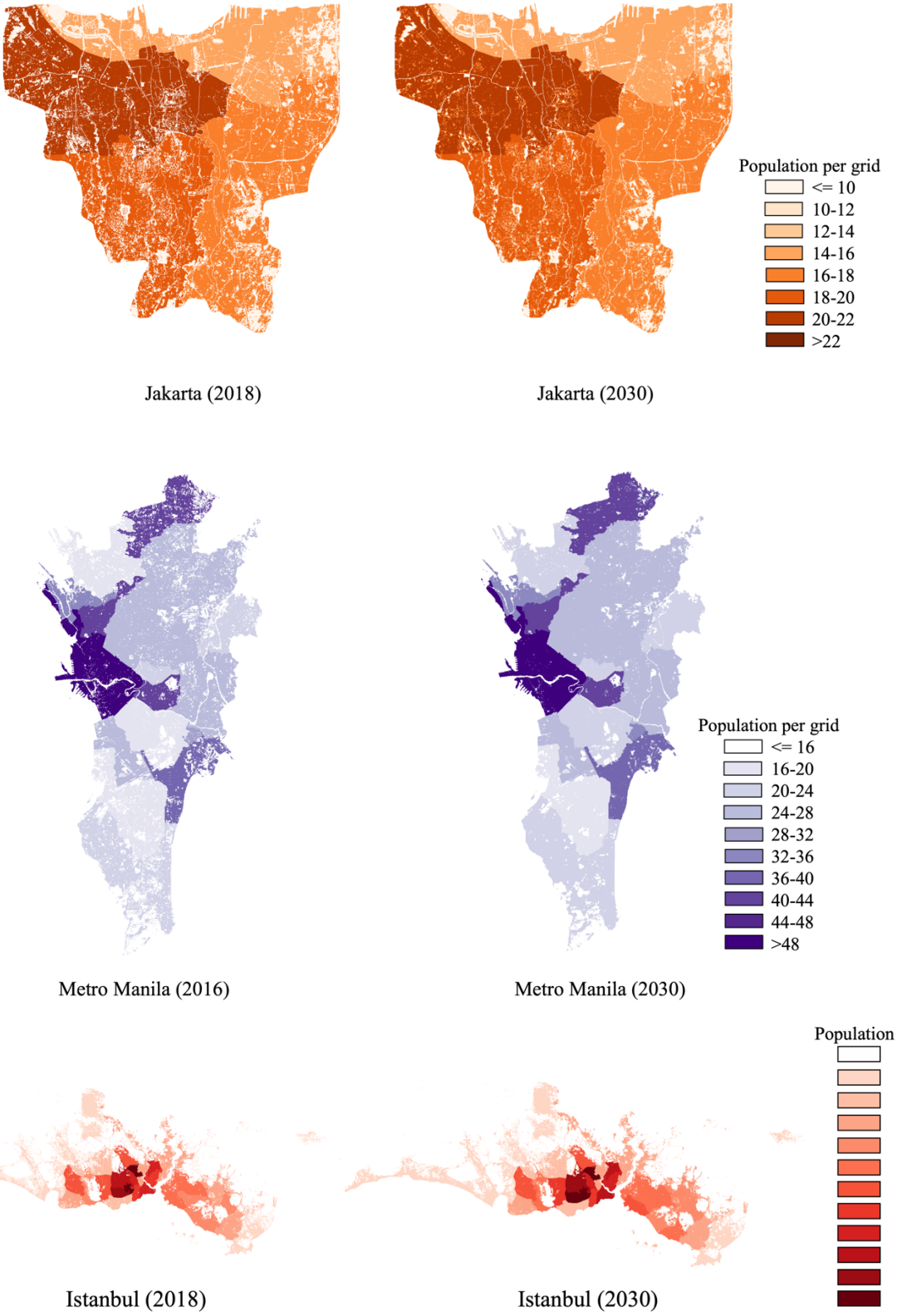


Fig. 4 – Population density maps representing present and future exposure



© The 17th World Conference on Earthquake Engineering 




## 2.3 Probabilistic Seismic Hazard Maps

Using the OpenQuake-engine developed by the Global Earthquake Model (GEM) Foundation [26] along with earthquake models of Southeast Asia [27] and Middle East [28], seismic hazard maps for 10% and 2% probabilities of exceedance (PoE) in 50 years were obtained. Soil amplification was also taken into consideration during this process utilizing $Vs_{30}$ (the average shear-wave velocity for the upper 30-m depth) values from the U.S. Geological Survey Database [29]. After obtaining the PGA values (Fig.5), they were converted to Modified Mercalli Intensity (MMI) scale as summarized in Table 2 [30]. It was observed that for 10% PoE in 50 years, Jakarta and Istanbul are subjected to MMI VII (Moderate) and MMI VIII (Moderate/Heavy) levels while Metro Manila is subjected to MMI VIII (Moderate/Heavy) and MMI IX (Heavy) levels. For 2% PoE in 50 years, Jakarta and Istanbul are subjected to MMI VIII (Moderate/Heavy) and MMI IX (Heavy) levels, and Metro Manila is subjected to only MMI IX (Heavy) level.

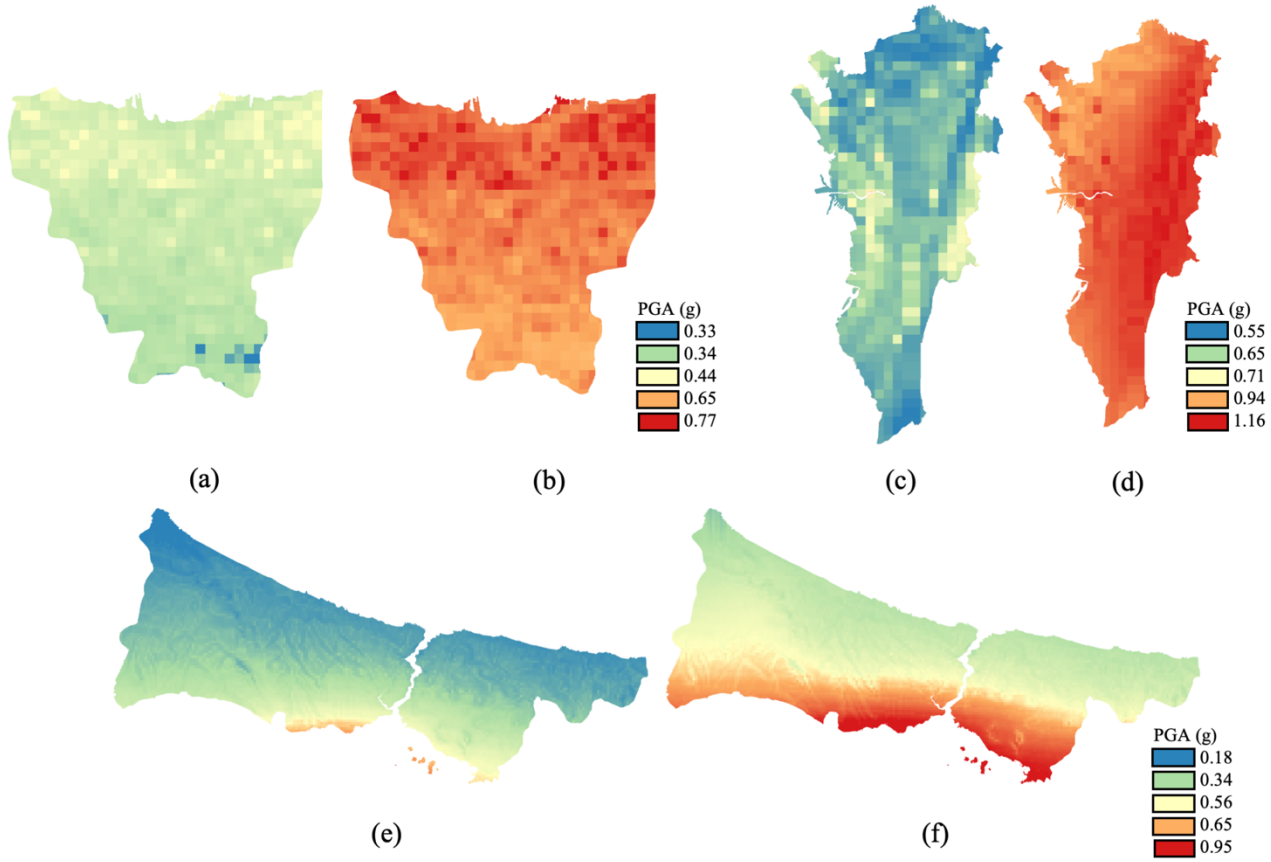


Fig. 5 – Seismic hazard maps in terms of PGA (g) for (a) 10% PoE in 50 years in Jakarta, (b) 2% PoE in 50 years in Jakarta (c) 10% PoE in 50 years in Metro Manila (d) 2% PoE in 50 years in Metro Manila (e) 10% PoE in 50 years in Istanbul, and (f) 2% PoE in 50 years in Istanbul

Table 2 – Conversion of PGA to MMI [30]

| Potential Damage | Moderate | Moderate/Heavy | Heavy |
|---|---|---|---|
| PGA (%g) | 18-34 | 34-65 | 65-124 |
| MMI | VII | VIII | IX |



© The 17th World Conference on Earthquake Engineering 



## 3. Results and Discussion

Seismic hazard maps were overlaid with the population density maps to obtain the population exposed to seismic hazard for different MMI levels. The population exposure (in million) and ratio to total population (%) for 10% and 2% PoE in 50 years are summarized in Table 3. The change in exposure from present to future is represented with bar charts in Fig.6 and Fig.7. As discussed above, 2018 is used to represent present for Jakarta and Istanbul while 2016 is used for Metro Manila due to data availability.

Table 3 – Population exposure (in million) and ratio to total population (%)

| | **MMI (Potential Damage)** | **Jakarta** | | **Metro Manila** | | **Istanbul** | |
|---|---|---|---|---|---|---|---|
| | | **2018** | **2030** | **2016** | **2030** | **2018** | **2030** |
| **10% PoE in 50 years** | **VII (Moderate)** | 0.16 (1.5%) | 0.20 (1.7%) | - | - | 1.88 (12.5%) | 2.43 (13.8%) |
| | **VIII (Moderate/High)** | 10.33 (98.5%) | 11.80 (98.3%) | 10.36 (79.2%) | 12.32 (79.6%) | 13.18 (87.5%) | 15.20 (86.2%) |
| | **IX (High)** | - | - | 2.72 (20.8%) | 3.16 (20.4%) | - | - |
| **2% PoE in 50 years** | **VIII (Moderate/High)** | 0.69 (6.6%) | 0.84 (7%) | - | - | 3.99 (26.5%) | 4.95 (28.1%) |
| | **IX (High)** | 9.80 (93.4%) | 11.16 (93%) | 13.08 (100%) | 15.48 (100%) | 11.07 (73.5%) | 12.68 (71.9%) |

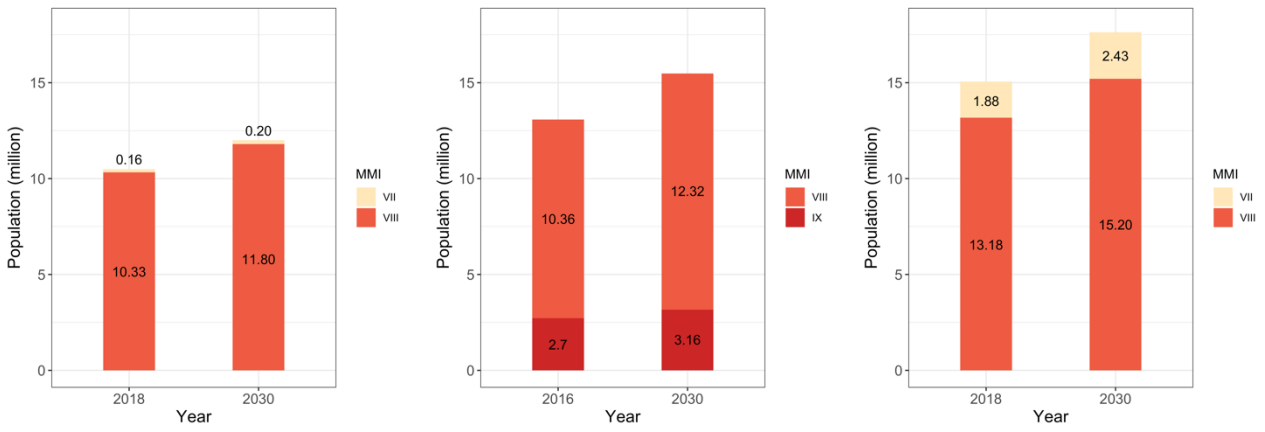


(a) Jakarta (b) Metro Manila (c) Istanbul

Fig. 6 – Population exposure to different MMI levels for 10% PoE in 50 years



© The 17th World Conference on Earthquake Engineering 




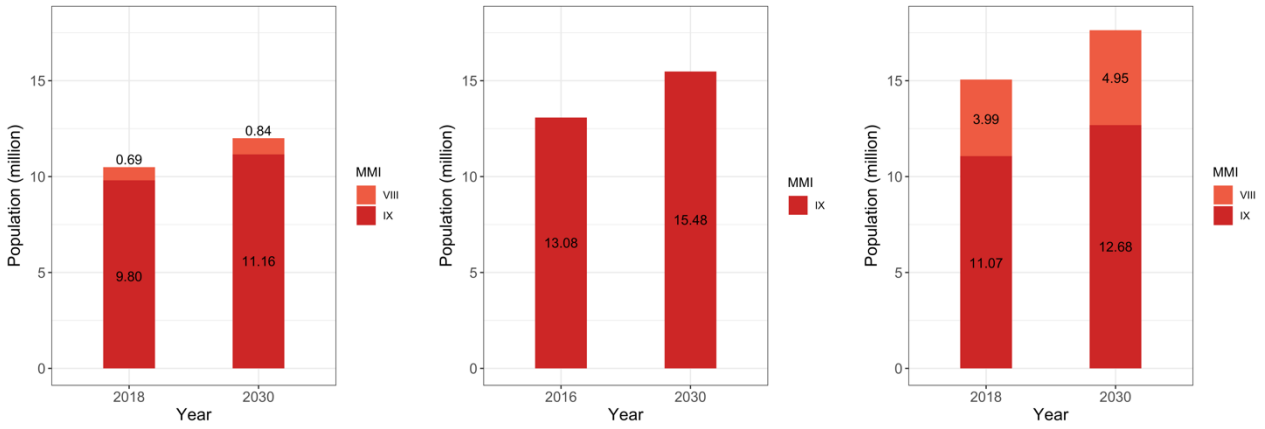


(a) Jakarta (b) Metro Manila (c) Istanbul

Fig. 7 – Population exposure to different MMI levels for 2% PoE in 50 years

For 10% probability of exceedance, most of the people in three megacities are subjected to MMI VIII (Moderate/Heavy) level. The number of people at this level is predicted to increase from 10.33 million to 11.80 for Jakarta, from 10.36 million to 12.32 million for Metro Manila, and from 13.18 million to 15.2 million for Istanbul. Although the ratio of population subjected to MMI VIII to total population is predicted to slightly increase for Metro Manila (from 79.2% to 79.6%), it is predicted to decrease for Jakarta (from 98.5% to 98.3%) and Istanbul (from 87.5% to 86.2%). The number of people subjected to MMI VII (Moderate) level is predicted to show a slight increase from 0.16 million to 0.20 million in Jakarta while there is a higher increase from 1.88 million to 2.43 million in Istanbul. For MMI IX (Heavy) level in Metro Manila, population is predicted to increase from 2.72 million to 3.16 million while the ratio to total population is predicted to show a slight decrease.

For 2% probability of exceedance, Istanbul and Jakarta are exposed to two MMI levels, namely MMI VIII (Moderate/Heavy) and MMI IX (Heavy) while Metro Manila has only MMI IX (Heavy) level as discussed above. Therefore, total population of Metro Manila is exposed to MMI IX level while an increase from 13.08 million to 15.48 million is predicted from 2016 to 2030. For Jakarta, around 93% of the total population is exposed to MMI IX level for both present (9.8 million) and future (11.16 million). Although this ratio is lower (around 70%) for Istanbul, the absolute number of people subjected to this level is higher when compared with Jakarta. It is predicted that there will be an increase from 3.99 million to 4.95 million, and from 11.07 million to 12.86 million in Istanbul for MMI VIII and MMI IX levels, respectively. For Jakarta, a slight increase is predicted from 0.69 million to 0.84 million for population subjected to MMI VIII level.

Our results demonstrate that the urban growth trends of all selected megacities are different as all have experienced different urbanization trends in the past. In Table 4, the increase in population exposure and the growth rates for different MMI levels are summarized. From the results, it is clear that the different exposure growth rates were obtained for different MMI levels in all megacities. Although the northern part of Istanbul has lower PGA values, the predicted increase in overall built-up area was observed to be high due to recent infrastructural developments in this region. Therefore, the growth rate of population exposure in Istanbul is higher in lower MMI levels. As opposed to similar urbanization patterns in Jakarta and Metro Manila, the pace of increase in population at risk is different for these two megacities. In MMI VIII level, the predicted increases in population values by 2030 are in descending order, 2.02 million for Istanbul, 1.94 million in Metro Manila and 1.5 million in Jakarta for 10% PoE in 50 years. For 2% PoE in 50 years, Metro Manila shows the highest population increase in MMI IX (2.4 million) while it is followed by Istanbul (1.61 million) and Jakarta (1.36 million). Although Istanbul's current population (~17.6 million) is relatively higher than Metro Manila (~15.5 million), predicted population exposure increase subjected to MMI IX (for 2% PoE in 50 years) is higher in Metro Manila when compared with Istanbul. These findings confirm the necessity of using spatio-temporal approaches for quantification of future seismic exposure.



© The 17th World Conference on Earthquake Engineering 



Table 4 – Changes in population exposure (in million) and growth rates (%) for different MMI levels

| | MMI | Jakarta | Metro Manila | Istanbul |
|---|---|---|---|---|
| **10% PoE in 50 years** | **VII** | 0.04 (25%) | - | 0.55 (29%) |
| | **VIII** | 1.5 (15%) | 1.94 (19%) | 2.02 (15%) |
| | **IX** | - | 0.44 (16%) | - |
| **2% PoE in 50 years** | **VIII** | 0.15 (22%) | - | 0.96 (24%) |
| | **IX** | 1.36 (14%) | 2.4 (18%) | 1.61 (15%) |

## 4. Limitations and Future Work

The approach that we present suffers from several limitations. First of all, there is a high level of uncertainty in the future population projections. We focus mainly on the administrative Level 2; however, there is a lack of data to make more accurate projections for this level. Because of this limitation, we used the overall megacity populations for projections that show more prominent temporal trends. For Jakarta and Metro Manila, the census populations are reported nearly every 5 years which again results in a limited number of data points for regression. To validate our findings, comparisons with demographic projections can be utilized in future studies. Secondly, our assumption about the maximum number of people to be allocated to the newly urbanized cells should be addressed in further studies. There might be cases in which the newly urbanized cells accommodate more people than the already urban cells. Another major source of limitation is the lack of information about the temporal trends of population allocation to the grids which have already been urban. In our study, total population values were adjusted to match the population projections obtained from linear regression. For this process, we scaled all cells (already urban and newly urbanized) in Metro Manila and Istanbul assuming they will be subjected to the same level of growth. Moreover, we scaled just the newly urbanized cells in Jakarta as the predicted population value after aggregation was higher than what was obtained from linear regression. Future studies could investigate the relation between urbanization and population growth in selected megacities to have more insight on these limitations.

## 5. Concluding Remarks

Population exposure to seismic hazard in Asia has been increasing rapidly as a result of recent urbanization. Megacities with a high concentration of people are heavily affected by this increase. In this study, we selected three Asian megacities, namely Jakarta, Metro Manila and Istanbul, to predict their future population exposure to seismic hazard, and to estimate the changes in exposure from present to future. The urban growth model SLEUTH was used to predict the spatio-temporal change of built-up area which was followed by disaggregation of extrapolated census population to the newly urbanized grids. Seismic hazard maps for 10% and 2% probabilities of exceedance were overlaid with population density maps, and the number of people subjected to different MMI levels were calculated for each megacity for the present and future. We found that the number of people subjected to MMI VIII (Moderate/Heavy) level for 10% PoE in 50 years is predicted to increase from 10.3 million to 11.8 million in Jakarta, from 10.4 million to 12.3 million in Metro Manila, and from 13.2 million to 15.2 million in Istanbul by 2030. For 2% PoE in 50 years, the population subjected to MMI IX (High) level is predicted to increase from 9.8 million to 11.2 million in Jakarta, from 13.1 million to 15.5 million in Metro Manila, and 11.1 million to 12.7 million in Istanbul. As a result of following a spatio-temporal approach, we observed that the population subjected to different MMI levels show different growth trends in each megacity.

The core objective of our study was to present an approach to use open-source data for prediction of future population exposure to seismic hazard both spatially and temporally which can be utilized by urban planners, insurance industry and decision-makers for risk assessment, management and mitigation purposes. Conventional risk and exposure estimation methods generally use the census population data and global



© The 17th World Conference on Earthquake Engineering 



gridded population datasets; however, thanks to the developments in technology, open-source databases based on remote sensing can also be employed by risk analysts for more comprehensive studies. Thus, instead of using data with low spatial resolutions, built-up area maps can be used as ancillary data for population disaggregation. Taking spatio-temporal changes into consideration, it is possible to give more coherent information about the future exposure.

## 6. Acknowledgments

We would like to thank Dr. Chung-Han Chan for providing the Earthquake Model of Continental Southeast Asia.

## 7. References

[1] Wenzel F, Bendimerad F, Sinha R (2014): Megacities – Megarisks. *Earthquake Risk Reduction, Module 1, Reading 1,* World Bank Distance Learning.

[2] Cardona OD, van Aalst MK, Birkmann J, Fordham M, McGregor G, Perez R, Pulwarty RS, Schipper ELF, Sinh BT, (2012): Determinants of risk: exposure and vulnerability. *A Special Report of Working Groups I and II of the Intergovernmental Panel on Climate Change (IPCC)*, Cambridge University Press, Cambridge, UK, and New York, NY, USA, 65-108.

[3] Freire S, Aubrecht C (2012): Integrating population dynamics into mapping human exposure to seismic hazard. *Natural Hazards and Earth System Sciences*, **12**, 3533-3543.

[4] Pesaresi M, Ehrlich D, Kemper T, Siragusa A, Florczyk A, Freire S, Corbane C (2017): Atlas of the Human Planet 2017: Global Exposure to Natural Hazards.

[5] Jaiswal K, Wald DJ (2013): Estimating economic losses from earthquakes using an empirical approach. *Earthquake Spectra*, **29(1)**, 309–324.

[6] Silva V, Amo-Oduro D, Calderon A, Dabbeek J, Despotaki V, Martins L, Rao A, Simionato M, Viganò D, Yepes C, Acevedo A, Horspool N, Crowley H, Jaiswal K, Journeay M, Pittore M (2018): Global Earthquake Model (GEM) Exposure Map (version 2018.1). DOI: 10.13117/GEM-GLOBAL-EXPOSURE-MAP-2018.1

[7] Zhang A, Wang J, Jiang Y, Chen Y, Shi P (2018): Spatiotemporal changes of hazard intensity-adjusted population exposure to multiple hazards in Tibet during 1982-2015. *Int J Disaster Risk Sci*, **9**, 541-554.

[8] Liang P, Xu W, Ma Y, Zhao X, Qin L (2017): Increase of elderly population in the rainstorm hazard areas oh China. *International Journal of Environmental Research and Public Health*, **14**, 963 – 980.

[9] Mestav Sarica G, Zhu T, Pan T-C (2019): Flood Exposure of Shenzhen from Past to Future: A Spatio-Temporal Approach using Urban Growth Modeling. *Proceedings of the 7th Annual International Conferenc on Architecture and Civil Engineering*, 400–405.

[10] Peduzzi P, Chatenoux B, Dao H, De Bono A, Herold C, Kossin J, Mouton, Nordbeck O (2012): Global trends in tropical cyclone risk. *Nature Climate Change*, **2**, 289-294.

[11] Hallegatte S, Green C, Nicholls RJ, Corfee-Morlot J (2013): Future flood losses in major coastal cities. *Nature Climate Change*, **3**, 802–806. https://doi.org/10.1038/nclimate1979

[12] Jones B, O'Neill B, McDaniel L, McGinnis S, Mearns LO, Tebaldi C (2015): Future population exposure to US heat extremes. *Nature Climate Change*, **5**, 652–655. https://doi.org/10.1038/nclimate2631

[13] Murnane RJ, Daniell JE, Schäfer AM, Ward PJ, Winsemius H, Simpson A, Tijssen A, Toro J (2017): Future scenarios for earthquake and flood risk in Eastern Europe and Central Asia. *Earth's Future*, **5**, 693–714, doi:10.1002/2016EF000481.

[14] Ehrlich D, Kemper M, Pesaresi M, Corbane C (2018): Built-up area and population density: Two essential societal variables to address climate hazard impact. *Environmental Science and Policy*, **90**, 73-82.

[15] Freire S, Aubrecht C, Wegscheider S (2013): Advancing tsunami risk assessment by improving spatio-temporal population exposure and evacuation modeling. *Natural Hazards*, **68**, 1311-1324.



© The 17th World Conference on Earthquake Engineering 




[16] Foresight Reducing Risks of Future Disasters: Priorities for Decision Makers (2012): Final Project Report. The Government Office for Science, London.

[17] Center for International Earth Science Information Network - CIESIN - Columbia University (2016): Gridded Population of the World, Version 4 (GPWv4): Population Count. Palisades, NY: NASA Socioeconomic Data and Applications Center (SEDAC). http://dx.doi.org/10.7927/H4X63JVC

[18] Lloyd C, Sorichetta A, Tatem A (2017): High resolution global gridded data for use in population studies. *Sci Data* **4**, 170001. https://doi.org/10.1038/sdata.2017.1

[19] Rose AN, McKee JJ, Urban ML, Bright EA (2018): LandScan 2017, Oak Ridge, TN, Oak Ridge National Laboratory.

[20] Silva EA, Clarke KC (2002): Calibration of the SLEUTH urban growth model for Lisbon and Porto, Portugal. *Computers, Environment and Urban Systems*, **26,** 525–552.

[21] Congedo L (2016): Semi-Automatic Classification Plugin Documentation, Release 5.3.6.1. http://dx.doi.org/10.13140/RG.2.2.29474.02242/1

[22] Statistics Indonesia, https://www.bps.go.id/ [accessed January 2019]

[23] Philippine Statistics Authority, https://psa.gov.ph/ [accessed January 2019]

[24] Turkish Statistical Institute, http://www.tuik.gov.tr/ [accessed January 2019]

[25] Pesaresi M, Melchiorri M, Siragusa A, Kemper T (2016): Atlas of the Human Planet 2016: Mapping Human Presence on Earth with the Global Human Settlement Layer.

[26] Pagani M, Monelli D, Weatherill G, Danciu L, Crowley H, Silva V, Henshaw P, Butler L, Nastasi M, Panzeri L, Simionato M, Vigano D (2014): OpenQuake Engine: An Open Hazard (and Risk) Software for the Global Earthquake Model. *Seismological Research Letters,* **85 (3),** 692–702.

[27] Chan C-H, Wang Y, Shi X, Ornthammarath T, Warnitchai P, Kosuwan S, Thant M, Nguyen PH, Nguyen LM, Solidum JrR, Irsyam M, Hidayati S, Sieh K (2017): Toward uniform probabilistic seismic hazard assessments for Southeast Asia. *2017 AGU Fall Meeting*.

[28] Giardini D, Danciu L, Erdik M, Sesetyan K, Demircioglu M, Akkar S, Gulen L, Zare M (2016): Seismic Hazard Map of the Middle East. Available from: http://www.seismo.ethz.ch [accessed February 2019]

[29] Wald DJ, Allen TI (2007): Topographic slope as a proxy for seismic site conditions and amplification. *Bulletin of the Seismological Society of America*, **97(5)**, 1379-1395

[30] Wald DJ, Quintoriano V, Heaton TH, Kanamori H (1999): Relationships Between Peak Ground Acceleration, Peak Ground Velocity, and Modified Mercalli Intensity in California. *Earthquake Spectra,* **15**, 557-564



© The 17th World Conference on Earthquake Engineering 